An Elevated Free Cytosolic Ca^{2+} Wave Follows Fertilization in Eggs of the Frog, *Xenopus laevis*

WILLIAM B. BUSA and RICHARD NUCCITELLI
Department of Zoology, University of California, Davis, California 95616

ABSTRACT The eggs of most or all animals are thought to be activated after fertilization by a transient increase in free cytosolic Ca^{2+} concentration ($[Ca^{2+}]_i$). We have applied Ca^{2+}-selective microelectrodes to detect such an increase in fertilized eggs of the frog, *Xenopus laevis*. As observed with an electrode in the animal hemisphere, $[Ca^{2+}]_i$ increased from 0.4 to 1.2 μM over the course of 2 min after fertilization, and returned to its original value during the next 10 min. No further changes in $[Ca^{2+}]_i$ were detected through the first cleavage division. In eggs impaled with two Ca^{2+} electrodes, the Ca^{2+} pulse was observed to travel as a wave from the animal to the vegetal hemisphere, propagating at a rate of ~10 μm/s across the animal hemisphere. The apparent delay between the start of the fertilization potential and initiation of the Ca^{2+} wave at the sperm entry site as ~1 min. Though these observations describe only the behavior of subcortical $[Ca^{2+}]_i$, we suggest that our data represent the subcortical extension of the cortical Ca^{2+} wave thought to trigger cortical granule exocytosis, and we present evidence that both the timing and magnitude of the Ca^{2+} pulse we observed are consistent with this identity. This first quantification of subcortical $[Ca^{2+}]_i$ during fertilization indicates that the Ca^{2+} transient is available to regulate processes (e.g., protein synthesis) in the subcortical cytosol.

The calcium theory of egg activation, which holds that an increase in free cytosolic Ca^{2+} concentration ($[Ca^{2+}]_i$)[1] sets in motion the early events of the "program of fertilization" (e.g., see reference 34), is amply supported by a variety of studies (2, 5–7, 10, 13, 14, 23, 27, 28, 37, 38). Qualitative measurements of $[Ca^{2+}]_i$ changes after fertilization in eggs of the medaka fish (14, 23), sea urchin (7, 28), starfish (7*a*), and mouse (6), with the use of the microinjected Ca^{2+}-sensitive photoprotein aequorin, have demonstrated a transient $[Ca^{2+}]_i$ increase after fertilization in all these eggs, and for the medaka, starfish, and sea urchin eggs have shown the $[Ca^{2+}]_i$ increase to traverse the egg as a wave (7, 7*a*, 14). Unfortunately, the aequorin technique can at best yield only estimates of $[Ca^{2+}]_i$ (such estimates for peak levels range from 1 μM in the sea urchin egg to 30 μM in the medaka egg), and cannot usually address the radial extent (cortical vs. subcortical) of the $[Ca^{2+}]_i$ increase. To clarify these points for the frog egg, and to determine whether wavelike $[Ca^{2+}]_i$ increases might be a general feature of egg activation, we have used Ca^{2+}-selective microelectrodes to study the response of *Xenopus laevis* eggs to fertilization.

[1] *Abbreviations used in this paper:* AH, animal hemisphere; $[Ca^{2+}]_i$, free cytosolic Ca^{2+} concentration; SES, sperm entry site; VH, vegetal hemisphere.

MATERIALS AND METHODS

Procurement and Handling of Gametes: Mature *Xenopus* oocytes were squeezed from females induced to ovulate via subcutaneous injection of 800–1,000 IU of human chorionic gonadotropin (Sigma Chemical Co., St. Louis, MO) on the previous night. Sperm were prepared by mincing dissected testes in F1 solution (see below). To prevent prick activation, eggs were impaled in F1 that contained 10 mM chlorobutanol, which was replaced with regular F1 just before insemination. F1 solution was prepared as previously described (17). Experiments were conducted at room temperature, between 20.5 and 24°C.

Fabrication of Microelectrodes: Our Ca^{2+} electrodes were a modified version of those of Tsien and Rink (31, 32). Chromic acid–cleaned borosilicate glass micropipettes without an inner fiber were broken to ~2-μm tip diameter and rendered hydrophobic by baking for 30 min at 200°C in a chamber that contained tri-*N*-chlorobutylsilane (Pfaltz & Bauer Inc., Stamford, CT) vapor in air. The pipettes were then backfilled with pCa 7 calibration buffer (see below) by applying gentle pressure from a syringe to the back end of the pipettes, then the tips were filled via suction with a 50–100-μm column of ungelled Ca^{2+} sensor, prepared as previously described (31). Finally, the electrode tips were briefly dipped twice into poly(vinyl chloride)–gelled Ca^{2+} sensor (32) and dried at 45°C for 15 min after each dip. All Ca^{2+} sensor components were purchased from Fluka Chemical, Hauppauge, NY. Average 90% response time from pCa 6.5 to 6 was 8 s (SD = 4 s, n = 7); at higher Ca^{2+} levels, response was typically even faster. Response slopes ranged from 20–29 mV between pCa 6 and 7.

Membrane potential microelectrodes with submicrometer tips were pulled from borosilicate glass tubing that contained an inner fiber, and were backfilled with 0.5 M KCl, 10 mM EGTA (pH 7.4). Their resistance ranged from 7 to 15 megaohms in F1.

Electrophysiological Recording: Experiments were performed in a 3-mm-deep plexiglass and glass chamber through which solutions were pumped intermittently by hand. The bath was grounded via an Ag/AgCl electrode in an Fl agar-filled tube. Membrane potential electrode output was amplified by a standard electrophysiological amplifier; Ca^{2+} electrode output was connected to a unity gain, high input impedance Analog Devices 311J amplifier. Subtraction of membrane potential from the Ca^{2+} electrode output was performed at the chart recorder.

Ca^{2+} electrodes were calibrated in buffers of pCa 6, 6.5, and 7 (negative log of free Ca^{2+} concentration). These contained 10 mM EGTA, 5 mM $CaCl_2$, and (for pCa 6) 10 mM PIPES, 45 mM KOH, 15 mM KCl (pH 6.77 at 23°C); (for pCa 6.5) 10 mM PIPES, 47 mM KOH, 12 mM KCl (pH 7.02 at 23°C); (for pCa 7) 10 mM 4-morpholinepropanesulfonic acid, 35.5 mM KOH, 29.3 mM KCl (pH 7.27 at 23°C). These buffers' ionic strength was 75 mM, close to that of *Xenopus* egg cytosol (see reference 36). We used the "mixed constants" for EGTA of Martell and Smith (20) to calculate the resulting free Ca^{2+} levels after correction for ionic strength as discussed on page 45 of reference 30. Electrodes were calibrated before and after cell impalement; only data from those displaying nearly identical recalibrations after impalement were used for the quantification of $[Ca^{2+}]_i$ (~25% of electrodes met this criterion).

Cell impalement with the membrane potential electrode was performed by increasing the negative capacitance; impalement with the blunter Ca^{2+} electrodes required a sharp tap on the end of the electrode holder with a forceps handle.

Determination of Ca^{2+} Wave Velocity: Eggs impaled in the animal hemisphere (AH) with two Ca^{2+} electrodes (one near the animal pole, the other near the equator) were photographed ~15 min after fertilization, after relaxation of the cortical contraction. The sperm entry site (SES) was visible as a localized accumulation of pigment. Planar coordinates of the SES and impalement sites taken from these photos were converted to three-dimensional coordinates on the egg surface, and the direction cosines a, b and c of each site were calculated as

$$\cos a = x/\sqrt{x^2 + y^2 + z^2},$$

$$\cos b = y/\sqrt{x^2 + y^2 + z^2},$$

and

$$\cos c = z/\sqrt{x^2 + y^2 + z^2},$$

where x, y and z are the coordinates of the site. The angle, θ, with vertex at the origin, between two points on a sphere is described by the relation

$$\cos \theta = \cos a_1 \cos a_2 + \cos b_1 \cos b_2 + \cos c_1 \cos c_2,$$

where the subscripts 1 and 2 refer to the two points. From calculated values of θ and the measured radius of the egg, the circumferential distance between each impalement site and the SES was determined. Assuming that the SES is the initiation site of the Ca^{2+} wave (as in medaka) and that the wave propagates at approximately constant velocity in all directions, this velocity is then $V = (D_b - D_a)/T_{a,b}$, where a and b are the first and second electrodes to detect the Ca^{2+} pulse, respectively, D is the circumferential distance from the electrode to the SES, and $T_{a,b}$ is the interval between detection of the pulse at electrodes a and b. The apparent lag between onset of the fertilization potential and initiation of the Ca^{2+} wave at the SES is then $L = T_a - (D_a/V)$, where T_a is the interval between onset of the fertilization potential and detection of the Ca^{2+} wave at the first electrode. Electrode impalement depth was not taken into account in these analyses.

Statistical Analysis: All averages are expressed as the mean ± SEM. The significance of differences in Ca^{2+} wave characteristics between the two hemispheres of eggs were determined via Student's t test for paired data; Student's t test for unpaired data was used for all other comparisons. The criterion for significance was $P < 0.05$.

RESULTS

$[Ca^{2+}]_i$ Increases Threefold after Fertilization

Fig. 1 shows a typical result for an egg impaled with a Ca^{2+} electrode in the animal hemisphere. Upon washout of the 10 mM chlorobutanol present during impalement (to prevent prick activation), $[Ca^{2+}]_i$ increased to its resting level (pCa 6.32), reflecting the ability of chlorobutanol to reversibly depress $[Ca^{2+}]_i$ (see below). At fertilization, a typical depolarization of membrane potential, the "fertilization potential",

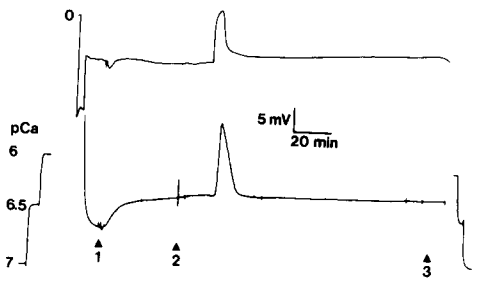

FIGURE 1 Membrane potential (*top*) and AH $[Ca^{2+}]_i$ in a fertilizing *Xenopus* egg. At *1*, chlorobutanol was removed from the bathing medium. At *2*, minced testis was added. At *3*, cleavage furrow formation began. Traces at the far left and right (*bottom*) are Ca^{2+} electrode calibrations at the indicated pCa levels.

was observed; 2.2 min after the onset of the fertilization potential, $[Ca^{2+}]_i$ began to increase rapidly (over 2.1 min) to 2.1 μM (pCa 5.68) and immediately began to recover, returning to its original value over the next 12 min. No further changes in $[Ca^{2+}]_i$ were observed in four eggs through the first cleavage division, in agreement with the observations of Rink et al. (24). In seven eggs from seven females, resting $[Ca^{2+}]_i$ before fertilization was 0.40 μM (pCa 6.4 ± 0.02), in good agreement with the resting pCa of 6.5 measured in 2–64-cell embryos (24). The mean peak $[Ca^{2+}]_i$ after fertilization was 1.2 μM (pCa 5.93 ± 0.06), and the final level after the Ca^{2+} pulse was 0.41 μM (pCa 6.39 ± 0.02), which is not significantly different from its prefertilization value.

Although we cannot specify precisely the depth of impalement achieved in these studies, we note that the values quoted clearly represent subcortical $[Ca^{2+}]_i$ levels. The morphologically defined cortex of the *Xenopus* egg is <5 μm thick (9), and its total radius is ~650 μm. Considerable force (delivered by tapping the end of the electrode holder) is required to achieve impalement with these rather blunt electrodes, driving the tip deeply into the egg. In three impalements, a ring of pigment granules could be seen adhering to the poly(vinyl chloride)–coated electrode shank after withdrawal; in each case this ring was ≥100 μm from the tip. We estimate that the average depth of impalement was on the order of 100 μm. Since impalement depth was uncontrolled, the small SE's listed above suggest that resting and peak Ca^{2+} levels do not depend sharply on depth, at least in the subcortical region.

The Increase In $[Ca^{2+}]_i$ Traverses the Egg as a Wave

To determine whether the Ca^{2+} pulse traverses the egg as a wave, we performed double impalements, with Ca^{2+} electrodes present simultaneously in both the pigmented animal hemisphere (AH) and unpigmented vegetal hemisphere (VH), approximately equidistant from the equator. Fertilization in frog eggs apparently occurs only in the AH (8); thus, a propagated wave of elevated $[Ca^{2+}]_i$ commencing at the sperm entry site (as observed in the medaka egg) should ordinarily be detected first by the AH electrode (except in the rare instance when the SES is equidistant from each electrode). In Fig. 2, the Ca^{2+} pulse is first detected in the AH 3.2 min after the onset of the fertilization potential, and in the VH some 2 min later. For eight eggs from eight females, the average delay between the AH and VH pulses was 1.9 ± 0.4 min, significant at the $P < 0.005$ level, demonstrating that the subcortical calcium pulse travels as a wave from AH to VH. The total

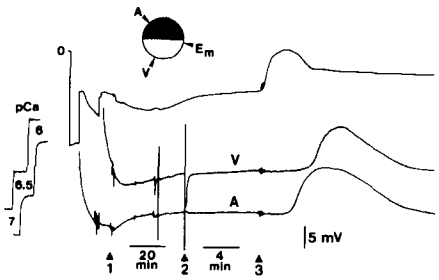

FIGURE 2 Membrane potential (*top*) and animal (*A*) and vegetal (*V*) hemisphere $[Ca^{2+}]_i$ during fertilization in a doubly-impaled egg. Inset shows approximate electrode placement with respect to the pigmented animal hemisphere. At *1*, chlorobutanol was removed. At *2*, minced testis was added and the chart recorder speed was increased as indicated. At *3*, artifacts due to poor subtraction of the membrane potential spikes at fertilization are visible in the *A* and *V* traces.

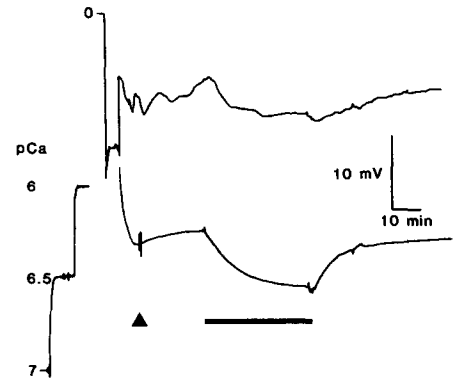

FIGURE 3 Membrane potential (*top*) and AH $[Ca^{2+}]_i$ (*bottom*) during chlorobutanol anesthesia of an unfertilized egg. Impalement was performed in FI containing 10 mM chlorobutanol, which was replaced by regular FI at the arrow. 10 mM chlorobutanol was reintroduced during the period indicated by the bar. This egg subsequently displayed a normal Ca^{2+} pulse after treatment with 10 μM A23187 (not shown).

duration of the wave (to 90% recovery) in the two hemispheres was not significantly different, lasting 10.3 ± 1.1 min in the AH and 10.0 ± 0.5 min in the VH, but the rise time of the AH wave (2.2 ± 0.3 min) was significantly shorter than that in the VH (3.0 ± 0.3 min; $P < 0.025$). This difference may reflect the lower density in the VH of junctions between the plasma membrane and cortical endoplasmic reticulum, as the cortical reticulum and its plasma membrane junctions have been suggested to be involved in Ca^{2+} release after fertilization (4, 12).

To determine the rate of propagation of the calcium wave, we performed experiments with two Ca^{2+} electrodes in the AH (to avoid the confounding effects of a possible difference in rate between the two hemispheres). For four experiments at 21–24°C (mean = 22°C) the mean velocity of the Ca^{2+} wave in the AH was 9.7 ± 1.5 μm/s, and the apparent delay between the fertilization potential and onset of the Ca^{2+} wave at the sperm entry site was 63 ± 5.5 s. In one experiment, the sperm entry site was located only 20 μm from the first Ca^{2+} electrode to detect the wave, yet the delay was still 64 s; this suggests that the "apparent" mean delay of 63 s accurately reflects the timing of this event.

Chlorobutanol Reversibly Depresses $[Ca^{2+}]_i$

Because impalement with our fairly blunt Ca^{2+} electrodes tended to activate eggs, all impalements discussed here were performed in F1 that contained 10 mM chlorobutanol, which has long been known to inhibit prick activation. We observed that upon washout of the chlorobutanol just before insemination, $[Ca^{2+}]_i$ typically increased by ~0.1 – 0.5 pCa unit, as seen in Figs. 1 and 2. Preliminary experiments such as that of Fig. 3 demonstrated that this reflects the ability of chlorobutanol to reversibly depress resting $[Ca^{2+}]_i$ (in this experiment by 0.3 pCa unit). Chlorobutanol had no effect on the electrode response in calibration buffers (data not shown).

DISCUSSION

New Findings

Our data extend the known instances of Ca^{2+} waves accompanying egg activation from the medaka (14), starfish (7*a*), and sea urchin (7) eggs to include the frog egg as well. Indeed, it has been suggested that Ca^{2+} waves are a ubiquitous feature of deuterostome egg activation (19), and our data support this hypothesis.

A unique contribution of the present study is our direct quantification of the resting and peak $[Ca^{2+}]_i$ in the subcortical cytosol of an activating egg. The medaka egg is somewhat unusual in that it is centrolecithal, with a 5–40 μm shell of cytoplasm surrounding a membrane-bounded yolk compartment which comprises the bulk of the cell. If one defines the cortex as the layer of cytoplasm that contains the cortical granules, then in this important respect the whole of the medaka egg cytoplasm is cortical. Further, Steinhardt et al. (28) tentatively concluded that the $[Ca^{2+}]_i$ increase they observed in sea urchin eggs via the aequorin technique was probably confined to the cortex. Hence, our data are the first to demonstrate that the $[Ca^{2+}]_i$ increase accompanying fertilization is available to regulate processes occurring in the subcortical region of the noncentrolecithal egg (e.g., protein synthesis; see reference 37).

Our use of Ca^{2+}-selective microelectrodes has also enabled us to detect the ability of chlorobutanol to reversibly lower $[Ca^{2+}]_i$. Because prick activation of *Xenopus* eggs requires extracellular Ca^{2+} (38), this observation immediately suggests a mechanism of action for chlorobutanol in inhibiting prick activation—i.e., by lowering $[Ca^{2+}]_i$ sufficiently, the leakage of extracellular Ca^{2+} into the egg through the prick wound cannot raise $[Ca^{2+}]_i$ to the triggering level necessary to initiate activation.

An unexpected result of this study was the surprisingly long apparent delay between the first observable sign of fertilization, the fertilization potential, and the onset of the Ca^{2+} wave at the sperm entry site. While we cannot rule out the possibility that the Ca^{2+} wave begins at the plasma membrane immediately after fertilization but requires 1 min to propagate (or diffuse?) to the subcortically located electrode tip, the recent report by Eisen et al. (7) of a 23-s delay between fertilization potential and onset of the Ca^{2+} transient (as observed via aequorin luminescence) in eggs of the sea urchin *Arbacia* suggests that the delay we observed is real. Several authors (14, 18, 25) have suggested that the fertilizing sperm initiates the Ca^{2+} pulse after sperm-egg fusion by delivering a bolus of sperm-derived Ca^{2+} to the egg cytosol at the sperm entry site, thus initiating Ca^{2+}-induced Ca^{2+} release, presumably from the endoplasmic reticulum. It seems difficult to comfortably accommodate a 1-min delay within such a scheme, since Ca^{2+}-induced Ca^{2+} release is an inherently rapid

process (at least in mammalian cardiac muscle; e.g., see reference 11). Thus, delays of the magnitude observed in the sea urchin and frog eggs suggest to us that, while the Ca^{2+} wave may well be propagated via Ca^{2+}-induced Ca^{2+} release, it is initiated by the sperm via another means involving a series of (time consuming) events. Recent observations by Turner et al. (33) of increased polyphosphoinositide turnover after fertilization suggest that this time-consuming sequence could involve activation of phospholipase C and its subsequent generation of inositol trisphosphate to trigger the Ca^{2+} wave (see *Note Added in Proof*).

The Form of the $[Ca^{2+}]_i$ Wave in the Xenopus Egg

Our data concerning the timing of the $[Ca^{2+}]_i$ wave permit a rough visualization of its form as it traverses the egg (Fig. 4), which can be useful in assessing its functions. We have assumed as a first approximation that the rate of propagation is roughly constant over the entire egg, and have applied the rate determined in the animal hemisphere to the vegetal hemisphere as well. In the medaka egg, the vegetal hemisphere propagation rate is, on average, 30% slower than that in the animal hemisphere (14). A similar retardation in the *Xenopus* egg would affect the absolute timing shown in the bottom row of Fig. 4, but would not greatly change the overall picture presented.

An outstanding difference between the previous results for the medaka egg (14) and those presented in Fig. 4 is that, only in the *Xenopus* egg, the whole of the cell is simultaneously involved in some phase of the $[Ca^{2+}]_i$ transient (Fig. 4, *f–h*). As we discuss below, the subcortical $[Ca^{2+}]_i$ changes we report probably parallel the cortical $[Ca^{2+}]_i$ wave presumed to activate cortical granule exocytosis. Other cortical events thought to be regulated by this same Ca^{2+} wave include a ring-shaped wave of plasma membrane permeability change (Kline, D., and R. Nuccitelli, manuscript in preparation) and the "activation waves," narrow rings of cortical contraction which propagate across the egg at activation (16, 29). An important consequence of the broad spatial extent of this wave is thus that future models of the mechanism(s) of Ca^{2+}-induced triggering of the (relatively narrow) "activation" and transcellular current waves must address the means whereby they are terminated at their trailing edges while $[Ca^{2+}]_i$ is still elevated, or even near its peak value (at least subcortically), in the same sector of the cell.

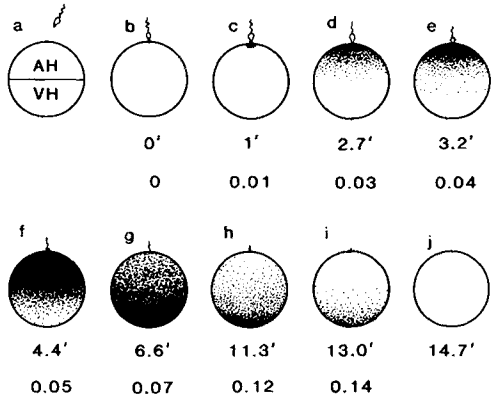

FIGURE 4 The approximate temporal sequence of events during the Ca^{2+} wave in a fertilized *Xenopus* egg, based on the data and assumptions discussed in the text. The approximate spacial extent and magnitude of increased $[Ca^{2+}]_i$ are indicated by the distribution and intensity of stippling, respectively. The first number beneath each drawing is the time, in minutes, from onset of the fertilization potential; the second number is the decimal fraction of the interval from fertilization potential to first cleavage at 22°C. Timing of sperm incorporation is arbitrary. (*a*) Orientation of egg, with animal pole at top. Fertilization is shown occurring there for simplicity. (*b*) Onset of fertilization potential. (*c*) Ca^{2+} wave begins at the sperm entry site. (*d*) Front of $[Ca^{2+}]_i$ wave reaches equator. (*e*) $[Ca^{2+}]_i$ peaks at sperm entry site. (*f*) Front of Ca^{2+} wave reached antipode. (*g*) $[Ca^{2+}]_i$ peaks at antipode. (*h*) Recovery complete at sperm entry site. (*i*) Recovery complete in animal hemisphere. (*j*) Recovery complete throughout cell.

Another significant difference between the results presented here and those previously reported for the medaka egg is the magnitude of the peak $[Ca^{2+}]_i$ level achieved. Gilkey et al. (14) estimated from their aequorin results a peak $[Ca^{2+}]_i$ of ~30 μM in the medaka egg, a 300-fold increase over the resting level. Due to the essentially qualitative nature of the aequorin assay, such estimates necessarily involve numerous assumptions, e.g., the volume of cytosol accessible to aequorin, the Ca^{2+} level in vivo at which aequorin luminescence is Ca^{2+}-independent, the intracellular free Mg^{2+} concentration, and the dependence of aequorin's light output on intracellular pH (since the nature of aequorin's pH-dependence, even in vitro, is a topic of debate; see references 1, 21, 26). Our direct quantification of $[Ca^{2+}]_i$ in the *Xenopus* egg yields a peak level of 1.2 μM, or a threefold increase over the resting level. In light of the 10,000-fold increase in aequorin luminescence in the activated medaka egg reported by Ridgway et al. (23), it may well be that the medaka egg, perhaps due to its centrolecithal structure, experiences a much larger Ca^{2+} transient than does the *Xenopus* egg. Alternatively, the assumptions involved in estimating peak $[Ca^{2+}]_i$ via the aequorin technique may lead to overestimates. In this regard, it is interesting to note that the $[Ca^{2+}]_i$ required to elicit cortical granule exocytosis in the medaka egg is between 2 and 5 μM at pH 7 (13), or just 7–17% of the peak $[Ca^{2+}]_i$ estimated by Gilkey et al. (14).

The Subcortical Ca^{2+} Wave May Be An Extension of a Similar Cortical Wave

In prick-activated *Xenopus* eggs, the front of cortical granule exocytosis begins almost instantly at the pricking site and propagates across the egg at a rate of ~9 μm/s (29). In fertilized eggs, a similar rate of propagation is observed (16, 29), but here the delay between fertilization and onset of exocytosis is unknown. It may be that pricking bypasses an initial step in sperm-induced egg activation (such as the generation of inositol trisphosphate discussed above), so that fertilization (but not pricking) could involve a delay similar to that which we observe; the important point is the approximate temporal correlation between the subcortical Ca^{2+} wave and exocytosis, as well as the good agreement in their rates of propagation. Further, the peak $[Ca^{2+}]_i$ level we observe is of the magnitude required to initiate cortical granule exocytosis. Using isolated cortices from eggs of the frog, *Rana pipiens*, Goldenberg and Elinson (15) observed breakdown of 50% of cortical granules at pCa 5.2 in medium of pH 6.4. In the medaka egg, the $[Ca^{2+}]$ which elicits cortical granule exocytosis is markedly pH-dependent (13), exactly reflecting the pH-dependence of the Ca^{2+} dissociation constant of calmodulin (3), the regula-

tory protein which has been implicated in control of cortical granule exocytosis in other eggs (27). Thus, we calculate that Goldenberg and Elinson's data, collected at a pH 1 unit lower than the intracellular pH of the *Xenopus* egg (22, 35, 36) probably overestimates the Ca^{2+} requirement for cortical granule exocytosis by 1 pCa unit (see reference 3 for discussion); i.e., the in vivo $[Ca^{2+}]_i$ required would be about pCa 6.2 (0.6 μM) at the low (~0.5 mM) Mg^{2+} concentration of *Xenopus* egg cytosol (35). If so, the peak $[Ca^{2+}]_i$ of 1.2 μM we report would be more than adequate to regulate this process. Thus, in both its timing and magnitude, the Ca^{2+} wave we report would coincide with that required to activate cortical granule exocytosis.

We thank Drs. K. Robinson and R. Y. Tsien for helpful discussions.

This was supported by National Science Foundation grant PCM 81 18174 and National Institutes of Health grant K04 HDO 0470-02 to R. Nuccitelli.

Received for publication 12 June 1984, and in revised form 21 December 1984.

Note Added in Proof: While this manuscript was in press, it was reported that microinjection of inositol-1,4,5-trisphosphate activates sea urchin eggs (Whitaker, M., and R. F. Irvine, 1984, *Nature (Lond.)*., 312:636–639). We have recently confirmed this with *Xenopus* eggs, and have shown that inositol-1,4,5-trisphosphate iontophoresis triggers a Ca^{2+} wave in these eggs that is identical to that reported in this paper (Busa, W. B., J. E. Ferguson, S. K. Joseph, J. R. Williamson, and R. Nuccitelli, manuscript submitted for publication).

REFERENCES

1. Baker, P. F., and P. Honerjager. 1978. Influence of carbon dioxide on level of ionised calcium in squid axons. *Nature (Lond.)*. 273:160–161.
2. Baker, P. F., and M. J. Whitaker. 1978. Influence of ATP and calcium on the cortical reaction in sea urchin eggs. *Nature (Lond.)*. 276:513–515.
3. Busa, W. B., and R. Nuccitelli. 1984. Metabolic regulation via intracellular pH. *Am. J. Physiol. 246 (Regulatory Integrative Comp. Physiol. 15)*:R409–R438.
4. Charbonneau, M., and R. D. Grey. 1984. The onset of activation responsiveness during maturation coincides with the formation of the cortical endoplasmic reticulum in oocytes of *Xenopus laevis*. *Dev. Biol.* 102:90–97.
5. Cross, N. L. 1981. Initiation of the activation potential by an increase in intracellular calcium in eggs of the frog, *Rana pipiens*. *Dev. Biol.* 85:380–384.
6. Cuthbertson, K. S. R., D. G. Whittingham, and P. H. Cobbold. 1981. Free Ca^{2+} increases in exponential phases during mouse oocyte activation. *Nature (Lond.)*. 294:754–757.
7. Eisen, A., D. P. Kiehart, S. J. Wieland, and G. T. Reynolds. 1984. Temporal sequence and spatial distribution of early events of fertilization in single sea urchin eggs. *J. Cell Biol.* 99:1647–1654.

7a. Eisen, A., and G. T. Reynolds. 1984. Calcium transients during early development in single starfish (*Asterias forbesi*) oocytes. *J. Cell Biol.* 99:1878–1882.

8. Elinson, R. P. 1975. Site of sperm entry and a cortical contraction associated with egg activation in the frog *Rana pipiens*. *Dev. Biol.* 47:257–268.
9. Elinson, R. P. 1980. The amphibian egg cortex in fertilization and early development. *In* The Cell Surface: Mediator of Developmental Processes. S. Subtelny and N. K. Wessells, editors. Academic Press, Inc., New York. 217–234.
10. Epel, D., C. Patton, R. W. Wallace, and W. Y. Cheung. 1981. Calmodulin activates NAD kinase of sea urchin eggs: an early event of fertilization. *Cell.* 23:543–549.
11. Fabiato, A., and F. Fabiato. 1979. Use of chlorotetracycline fluorescence to demonstrate Ca^{2+}-induced release of Ca^{2+} from the sarcoplasmic reticulum of skinned cardiac cells. *Nature (Lond.)*. 281:146–148.
12. Gardiner, D. M., and R. D. Grey. 1983. Membrane junctions in *Xenopus* eggs: their distribution suggests a role in calcium regulation. *J. Cell Biol.* 96:1159–1163.
13. Gilkey, J. C. 1983. Roles of calcium and pH in activation of eggs of the medaka fish, *Oryzias latipes*. *J. Cell Biol.* 97:669–678.
14. Gilkey, J. C., L. F. Jaffe, E. B. Ridgway, and G. T. Reynolds. 1978. A free calcium wave traverses the activating egg of the medaka, *Oryzias latipes*. *J. Cell Biol.* 76:448–466.
15. Goldenberg, M., and R. P. Elinson. 1980. Animal/vegetal differences in cortical granule exocytosis during activation of the frog egg. *Dev. Growth & Differ.* 22:345–356.
16. Hara, K., and P. Tydeman. 1979. Cinematographic observation of an "activation wave" (AW) on the locally inseminated egg of *Xenopus laevis*. *Wilhelm Roux's Arch. Dev. Biol.* 186:91–94.
17. Hollinger, T. G., and G. L. Corton. 1980. Artificial fertilization of gametes from the South African clawed frog, *Xenopus laevis*. *Gamete Res.* 3:45–57.
18. Jaffe, L. F. 1980. Calcium explosions as triggers of development. *Ann. NY Acad. Sci.* 339:86–101.
19. Jaffe, L. F. 1983. Sources of calcium in egg activation: a review and hypothesis. *Dev. Biol.* 99:265–276.
20. Martell, A. E., and R. M. Smith. 1974. Critical Stability Constants, Vol. 1. Plenum Publishing Corp., New York. 469 pp.
21. Moisescu, D. G., C. C. Ashley, and A. K. Campbell. 1975. Comparative aspects of the calcium-sensitive photoproteins aequorin and obelin. *Biochim. Biophys. Acta.* 396:133–140.
22. Nuccitelli, R., D. J. Webb, S. T. Lagier, and G. B. Matson. 1981. ^{31}P NMR reveals increased intracellular pH after fertilization in *Xenopus* eggs. *Proc. Natl. Acad. Sci. USA.* 78:4421–4425.
23. Ridgway, E. B., J. C. Gilkey, and L. F. Jaffe. 1977. Free calcium increases explosively in activating medaka eggs. *Proc. Natl. Acad. Sci. USA.* 74:623–627.
24. Rink, T. J., R. Y. Tsien, and A. E. Warner. 1980. Free calcium in *Xenopus* embryos measured with ion-selective microelectrodes. *Nature (Lond.)*. 283:658–660.
25. Schackmann, R. W., E. M. Eddy, and B. M. Shapiro. 1978. The acrosome reaction of *Strongylocentrotus purpuratus* sperm. Ion requirements and movements. *Dev. Biol.* 65:483–495.
26. Shimomura, O., and F. H. Johnson. 1973. Further data on the specificity of aequorin luminescence to calcium. *Biochem. Biophys. Res. Commun.* 53:490–494.
27. Steinhardt, R. A., and J. M. Alderton. 1982. Calmodulin confers calcium sensitivity on secretory exocytosis. *Nature (Lond.)*. 295:154–155.
28. Steinhardt, R., R. Zucker, and G. Schatten. 1977. Intracellular calcium release at fertilization in the sea urchin egg. *Dev. Biol.* 58:185–196.
29. Takeichi, T., and H. Y. Kubota. 1984. Structural basis of the activation wave in the egg of *Xenopus laevis*. *J. Embryol. Exp. Morph.* 81:1–16.
30. Thomas, M. V. 1982. Techniques in Calcium Research. Academic Press, Inc., New York. 214 pp.
31. Tsien, R. Y., and T. J. Rink. 1980. Neutral carrier ion-selective microelectrodes for measurement of intracellular free calcium. *Biochim. Biophys. Acta.* 599:623–638.
32. Tsien, R. Y., and T. J. Rink. 1981. Ca^{2+}-selective electrodes: a novel PVC-gelled neutral carrier mixture compared with other currently available sensors. *J. Neurosci. Methods.* 4:73–86.
33. Turner, P. R., M. P. Sheetz, and L. A. Jaffe. 1984. Fertilization increases the polyphosphoinositide content of sea urchin eggs. *Nature (Lond.)*. 310:414–415.
34. Tyler, A. 1941. Artificial parthenogenesis. *Biol. Rev. Camb. Philos. Soc.* 16:291–336.
35. Webb, D. J., and R. Nuccitelli. 1981. Direct measurement of intracellular pH changes in *Xenopus* eggs at fertilization and cleavage. *J. Cell Biol.* 91:562–567.
36. Webb, D. J., and R. Nuccitelli. 1982. Intracellular pH changes accompany the activation of development in frog eggs: comparison of pH-microelectrode and ^{31}P-NMR measurements. *In* Intracellular pH: Its Measurement, Regulation, and Utilization in Intracellular Functions. R. Nuccitelli and D. W. Deamer, editors. Liss, New York. 293–324.
37. Winkler, M. M., R. A. Steinhardt, J. L. Grainger, and L. Minning. 1980. Dual ionic controls for the activation of protein synthesis at fertilization. *Nature (Lond.)*. 287:558–560.
38. Wolf, D. P. 1974. The cortical response in *Xenopus laevis* ova. *Dev. Biol.* 40:102–115.